Journal of Electrochemistry

Volume 28
Issue 3 *Special Issue: Frontier of Electrochemistry (Ⅱ)*

2022-03-28

In Situ Characterization of Electrode Structure and Catalytic Processes in the Electrocatalytic Oxygen Reduction Reaction

Ya-Chen Feng

Xiang Wang

Yu-Qi Wang

Hui-Juan Yan

Dong Wang
1. CAS Key Laboratory of Molecular Nanostructure and Nanotechnology, Beijing National Laboratory for Molecular Science (BNLMS), Institute of Chemistry, Chinese Academy of Sciences, Beijing 100190, China;2. University of Chinese Academy of Sciences, Beijing 100049, China;, wangd@iccas.ac.cn

Recommended Citation

Ya-Chen Feng, Xiang Wang, Yu-Qi Wang, Hui-Juan Yan, Dong Wang. *In Situ* Characterization of Electrode Structure and Catalytic Processes in the Electrocatalytic Oxygen Reduction Reaction[J]. *Journal of Electrochemistry*, 2022 , 28(3): 2108531.
DOI: 10.13208/j.electrochem.210853
Available at: https://jelectrochem.xmu.edu.cn/journal/vol28/iss3/4

电 化 学
J. Electrochem. 2022, 28(3), 2108531 (1 of 13)

[Review] DOI: 10.13208/j.electrochem.210853 Http://electrochem.xmu.edu.cn

In Situ Characterization of Electrode Structure and Catalytic Processes in the Electrocatalytic Oxygen Reduction Reaction

Ya-Chen Feng[1,2], Xiang Wang[1,2], Yu-Qi Wang[1,2], Hui-Juan Yan[1,2], Dong Wang[1,2*]

(*1. CAS Key Laboratory of Molecular Nanostructure and Nanotechnology, Beijing National Laboratory for Molecular Science (BNLMS), Institute of Chemistry, Chinese Academy of Sciences, Beijing 100190, China; 2. University of Chinese Academy of Sciences, Beijing 100049, China*)

Abstract: As an electrochemical energy conversion system, fuel cell has the advantages of high energy conversion efficiency and high cleanliness. Oxygen reduction reaction (ORR), as an important cathode reaction in fuel cells, has received extensive attention. At present, the electrocatalysts are still one of the key materials restricting the further commercialization of fuel cells. The fundamental understanding on the catalytic mechanism of ORR is conducive to the development of electrocatalysts with the enhanced activity and high selectivity. This review aims to summarize the *in situ* characterization techniques used to study ORR. From this perspective, we first briefly introduce the advantages of various *in situ* techniques in ORR research, including electrochemical scanning tunneling microscopy, infrared spectroscopy, Raman spectroscopy, X-ray absorption spectroscopy, X-ray photoelectron spectroscopy and transmission electron microscopy. Then, the applications of various *in situ* characterization techniques in characterizing of the catalyst morphological evolution and electronic structure as well as the identification of reactants and intermediates in the catalytic process are summarized. Finally, the future development of *in situ* technology is outlooked.

Key words: oxygen reduction reaction; *in situ* characterization; electrocatalytic process

1 Introduction

As an important type of electrochemical energy conversion system, fuel cell is considered to be a promising clean energy device due to its high energy conversion efficiency, and other advantages[1-5]. The electrocatalyst is one of the key materials restricting the further commercialization of fuel cells[3-6, 7-10]. At present, Pt-based catalysts are still the most practical and effective type of electrocatalyst for fuel cells. Great efforts have been made to improve the catalytic efficiency and reduce the loading of the precious metal Pt, in order to reduce the cost of the fuel cell. On the other hand, the development of new Pt-free electrocatalysts, including M-N_x/C (M = Fe, Co, Ni, Mn, etc.)[6,11-13], transition metal oxides, has grown rapidly in recent years.

The electrocatalytic oxygen reduction reaction (ORR) is a multi-electron process involving multiple elementary steps and intermediate species. For example, it can be carried out by a direct four-electron reduction pathway, in which O_2 is adsorbed and dissociated on the catalyst surface, and then reduced to H_2O. On the other hand, the adsorbed O_2 can also form peroxide species through the process of electron and proton transfer, and then the peroxide diffuses into the solution or is further reduced to H_2O. An in-depth understanding of the mechanism and catalytic process of catalysts is of great significance for developing new and efficient electrocatalyst materials.

Traditional electrochemical methods and techniques,

Cite as: Feng Y C, Wang X, Wang Y Q, Yan H J, Wang D. *In situ* characterization of electrode structure and catalytic processes in the electrocatalytic oxygen reduction reaction. *J. Electrochem.*, 2022, 28(3): 2108531.

Received: 2021-11-24, Revised: 2022-02-05. *Corresponding author, Tel: (86-10)82616935, E-mail: wangd@iccas.ac.cn

such as cyclic voltammetry (CV)[14,15], rotating disk/ring electrode based electrochemical reaction dynamics study[16], electrochemical impedance spectroscopy[17,18], etc., can provide important information for electrochemical activity of catalyst and electrochemical reaction kinetics. Theoretical quantum mechanics calculations, such as density functional theory[19, 20], have been widely applied to analyze the electronic structure of electroactive sites and simulate the reaction kinetics. In this context, a molecular level or nanoscale characterization of the catalyst and the catalytic process (the morphology and electronic changes of the catalyst, intermediates in the catalytic process, etc.) by *in situ* techniques is valuable to provide comprehensive information about the reaction mechanism.

The advancement of surface characterization techniques provides a great opportunity to understand electrocatalytic processes. The key challenge is to adopt those surface characterization techniques into electrocatalytic compatible condition. In recent years, many efforts have been made to develop *in situ* technologies compatible with ORR. These technologies provide important *in situ* or *operando* information about electrocatalysts and catalytic processes. In revealing the details of the active electrocatalyst surface, *in situ* characterization techniques have been widely used to monitor the morphological evolution and electronic structure of the catalyst. For example, scanning tunneling microscopy (STM)[21-25] and transmission electron microscope (TEM)[26,27] have been used for the observation on the evolution of the catalyst surface morphology. *In situ* X-ray technology, such as X-ray absorption spectroscopy (XAS)[28-31], can provide information on the electronic structure and oxidation state of the catalyst. *In situ* X-ray diffraction (XRD)[41] technique is performed to detect the crystal phase of catalysts in real time. In addition to explore the dynamic evolution of the catalyst, the *in situ* characterization of the reactants and intermediate states in the ORR process is also crucial for understanding the catalytic mechanism. In this regard, STM can also provide information of reactant adsorption and electrocatalytic processes with atomic resolution. Infrared spectroscopy (IR)[32-35] and Raman spectroscopy (RS)[36-40] can detect vibration modes of the reaction intermediates sensitively.

This review summarizes the application of a variety of *in situ* technologies in the study of electrocatalytic ORR, focusing on the structure of electrocatalysts and surface catalytic processes. In addition, the challenges and future directions in the development of electrochemical *in situ* technology in the ORR field are also discussed.

2 Morphological Evolution and Electronic Structures of the Electrocatalyst

The catalysts play an important role in ORR. Using *in situ* characterization techniques to monitor the dynamic changes of the catalyst during the O_2 reduction process can help reveal the ORR mechanism. In this section, we will outline the use of *in situ* characterization techniques to study the evolution of the morphology and electronic structure of various catalysts during O_2 reduction.

2.1 Metal Catalysts

At present, Pt-based catalysts are still the most practical and effective electrocatalysts for ORR. Understanding the chemical state and morphological changes of Pt-based catalysts during ORR by advanced *in situ* techniques has attracted widespread attention.

XAS is a powerful technique for studying the electronic and chemical states of the catalysts. The technique is based on the transitions from the atomic core level to the unoccupied states in the valence band, providing element-specific information about the electronic structure and chemical states. *In situ* XAS can provide the average chemical information of the sample. The shape and intensity of the Pt L_3- and L_2-edge white lines (WLs) of XAS spectrum provide important information about the oxidation state of Pt and the species adsorbed on the surface. *In situ* XAS measurements were taken to uncover the oxidation state changes of model catalytic system using Pt particles under electrochemical environment in O_2-saturated 0.1 mol·L^{-1} $HClO_4$ solution[31]. As shown in Figure 1(A), the Pt K edge XAS spectra are obtained

at the different applied potentials. Figure 1(B) shows the trend of the peak area of the metal and oxidized components and their sum under the applied potential. The sum of the individual peak areas can be compared with the integrated white line intensity commonly used in XAS to indicate the oxidation state of platinum. At lower potentials (between 0 V and ~ 0.3 V vs. RHE), a broad asymmetric WL with a low intensity is observed, which is attributed to the adsorption of hydrogen on the catalyst surface (Pt-H). As the potential increases to between 0.3 and 0.96 V (vs. RHE), WL becomes narrow. The strength of the oxide component is essentially unchanged, while the strength of the metal component increases steadily, which is a characteristic of the increased coverage of chemically adsorbed oxygen species on the surface. When the potential is higher than 0.9 V (vs. RHE), WL width increases, and the strength of the metal component decreases, which means the conversion of metal Pt to PtO_x. Since the WL intensity of the catalyst in the final state (1.26 V vs. RHE) is lower than that of standard PtO_2, it indicates that the average oxidation state of Pt in the obtained PtO_x structure is lower than that of PtO_2.

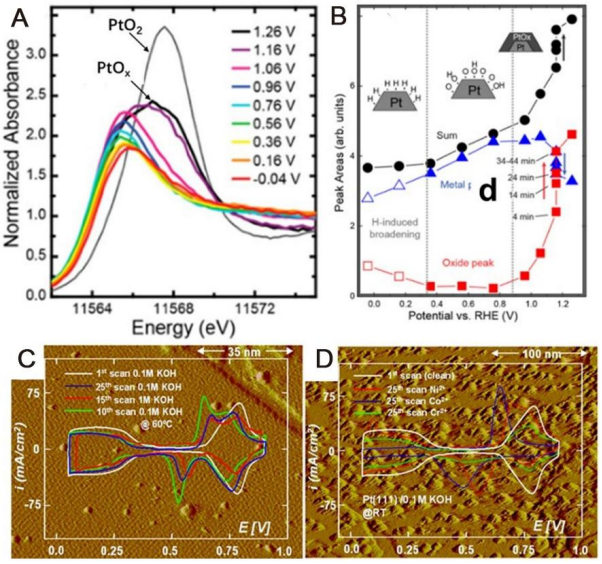

Figure 1 (A) Potential-dependent Pt L_3-edge XAS spectra of Pt NPs on a carbon support. (B) Evolution of the metallic, oxide and the total area of the catalyst as a function of the applied potential. (C) STM image of the as-prepared Pt(111) surface. (D) STM image of the Pt(111) electrode after the 25th sweep in 0.1 mol·L^{-1} KOH solutions containing Co^{2+}. (A-B) Reproduced from Ref[31]. With permission from the American Chemical Society. (C-D) Reproduced from Ref[21]. With permission from the American Chemical Society. (color on line)

STM is a real-time imaging technique with very high spatial resolution. The basic principle of STM is based on the tunneling effect between the atomically sharp metal tip and the conductive sample. By using the tunneling current as feedback, the tip is scanned over the surface to trace the structures of the electrode. STM can visualize the structural evolution of catalysts at the atomic scale, but it lacks chemical recognition ability. Subbaraman[21] et al. combined STM and CV to study the process of Pt surface catalyzed ORR as the model system. They found that in the process of catalytic oxygen reduction, transition metal ions form some hydroxide species on the Pt surface, which hinders the progress of the Pt surface catalyzed ORR, thereby reducing the catalytic activity of the Pt catalyst. They studied the changes of CV and STM in Co^{2+} and Co^{2+}-free electrolytes. As shown in Figure 1 (C, D), after doping with Co^{2+} ions and repeatedly scanning the CV for 25 cycles, the Pt surface becomes rough. Many cluster-like species can be classified as hydroxide products formed by transition metal ions on the surface of Pt during the catalytic ORR process.

The XRD technique is a general technique to characterize the crystalline structure of the materials. The *in situ* XRD technique can monitor the crystal phase of the catalyst in real time, and further analyze the phase transition of the catalysts. For reducing the cost and increasing the activity, alloy catalysts have been extensively investigated. For instance, Wu et al.[41] used *in situ* synchrotron high-energy XRD to probe the structural evolution of palladium nickel alloy electrocatalysts (PdNi). As shown in Figure 2(A), for $Pd_{30}Ni_{70}$, during the electrochemical potential cycle in the ORR operating potential window, the atom pair distribution function analysis of the distance between the bimetallic atoms presents an oscillating trend, but the bimetallic structure still exists. Figure 2(B) shows that the metallic Ni was partially leached and the Pd

content increased during multiple cycles, but the synergy between the two metals remained unchanged, and the catalytic activity also reached a peak when the Pd content reached 50%.

In situ TEM techniques are used to characterize the morphological changes of catalysts during the reaction. The *in situ* electrochemical cell inside a TEM chamber can enable direct monitoring of the morphological changes in the catalyst under electrode potential control. Zhu et al.[42] used *in situ* TEM to observe morphological changes of the Pt-Fe nanocatalyst at different potentials. As shown in Figure 2(C), the growth of nanoparticles can be observed under different potential cycles. These observations indicate that particles coalesce with neighboring particles to form irregular structures. The 150-cycle CV curve in Figure 2(D) is relatively stable and shows changes in the catalytic structure, such as the acid leaching of Fe from the Pt-Fe nanocatalyst and the coarsening of the nanocatalyst. Due to the hydrogen desorption on the active site of Pt, the characteristic peak at -0.2 V (vs. RHE) increased during 0 ~ 50 cycles and then decreased. During the forward scan, the metal oxidation peak initially appeared at 0.45 V (vs. RHE), and after 150 cycles, the oxidation peak potential became 0.9 V (vs. RHE) (black arrow). These observations imply that Pt active sites increase and then decrease during the cycle, which may be due to iron leaching to form a Pt-rich surface and subsequent coarsening of the nanoparticles.

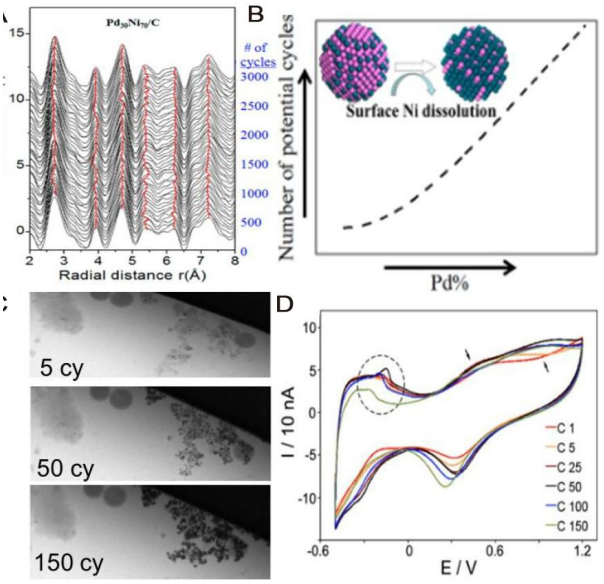

Figure 2 (A) *In situ* atomic PDFs for $Pd_{30}Ni_{70}$NPs obtained in a custom-built fuel cell cycled between 0.6 ~ 1.2 V (vs. RHE) at a scan rate of 100 mV·s^{-1}. (B) Trend for the change in composition of $Pd_{30}Ni_{70}$/C catalyst as a result of Ni-leaching during the potential cycling. (C) Morphologies of Pt-Fe nanocatalysts at additional 5th, 50th, and 150th cycles after the first 130 cycles. (D) The corresponding CV curves at 1st, 5th, 25th, 50th, 100th, and 150th cycles. (A-B) Reproduced from ref[41]. With permission from the American Chemical Society. (C-D) Reproduced from ref[42]. With permission from the American Chemical Society. (color on line)

2.2 Metal Oxides

XAS technique has also been used in the investigation of the electronic structure of the catalysts. As early as 1979, Brenet[43] proposed that Mn(III) would be oxidized and converted to Mn(IV) in the ORR process. Mao et al.[44] found that in 1.0 mol·L^{-1} KOH, the ORR catalyzed by Mn_yO_x is a continuous two-electron process, and $*O_2H$ is an intermediate species. Lima[29] et al. obtained the manganese oxide MnO_2 through thermal decomposition, and used *in situ* XANES to study the process of manganese oxide catalyzing ORR in an alkaline solution. The *in situ* XANES spectra obtained at different potentials are shown in Figure 3(A). With the change of electrode potential, the spectrum curve has changed a lot, indicating that the oxidation state of Mn has been changed strongly. By comparing the XANES spectra under different electrode potentials with Mn(II), (III) and (IV) standard manganese oxides (represented by MnO, MnOOH and MnO_2), it can be seen that at 0.40 V (vs. RHE), the catalyst is not reduced, and the original catalyst is mainly composed of MnO_2, which is consistent with the results obtained by XRD. Combined with the CV results, it is shown that when the electrode potential drops to -0.10 V (vs. RHE), Mn(IV) is reduced to Mn(III) and ORR is turned on. When the electrode potential is further reduced to -0.70 V (vs RHE), the sample is reduced to Mn(II). The results show that MnO_2 undergoes Mn(IV)/Mn(III) and Mn(III)/Mn(II) transitions in the catalyzing ORR process

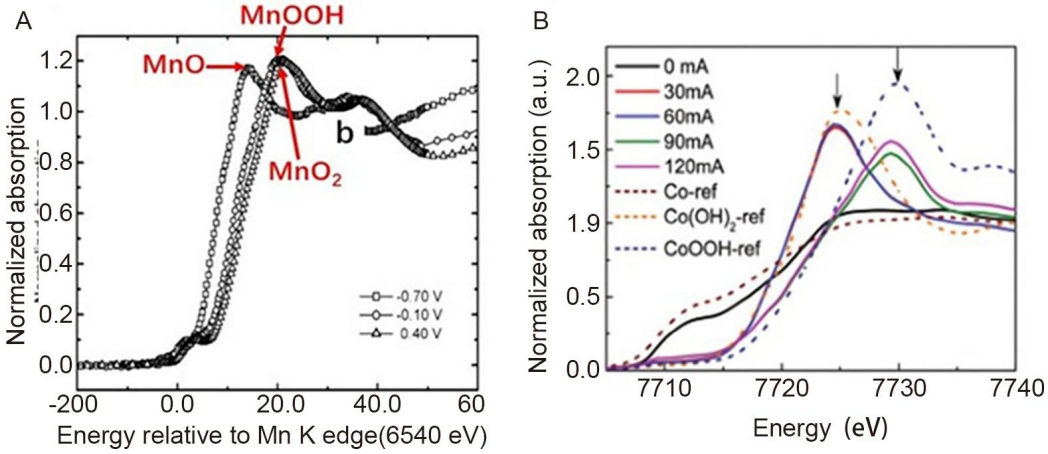

Figure 3 (A) *In situ* XANES spectra at the Mn K-edge for the MnO_2 at different electrode potentials in 1.0 mol·L^{-1} KOH. (B) *In situ* XANES spectra of the Co-PPy-BP cathode and standard Co, $Co(OH)_2$ and CoOOH samples. (A) Reproduced from ref[29]. With permission from the Elsevier. (B) Reproduced from ref[45]. With permission from the Royal Society of Chemistry. (color on line)

of MnO_2, where Mn(III) acts as an active site during ORR.

2.3 Molecular Catalysts

Qin[45] and colleagues studied the electrocatalytic performance of the PPy-modified carbon-supported cobalt-based catalyst (Co-PPy-BP). The *in situ* X-ray absorption near edge structure (XANES) spectrum of the Co-PPy-BP cathode is illustrated in Figure 3(B). Before the reaction, the XANES spectrum of Co-PPy-BP was similar to that of the standard Co sample. With the beginning of the ORR reaction, the XANES spectrum of Co-PPy-BP changed significantly, tending to be similar to that of the standard $Co(OH)_2$ sample. This means that when the ORR reaction is started, the catalyst Co-PPy-BP undergoes a transformation from Co^0 to Co^{2+}. As the reaction progresses, the XANES spectrum of Co-PPy-BP becomes similar to that of the standard CoOOH sample, which indicates that Co^{2+} is further converted to Co^{3+}. These analysis results indicate that Co(II) acts as an active site in the ORR catalysis process.

3 Investigation of Intermediates in Electrocatalytic Reaction

In addition to exploring the dynamic structure evolution of the catalyst, the *in situ* characterization of the reactant O_2 and other intermediates during the O_2 reduction process is also crucial for understanding the catalytic mechanism. In this section, we summarize the application of *in situ* characterization techniques in the detection of reactants O_2 and intermediates in the O_2 reduction process.

3.1 Metal Catalysts

In situ RS and *in situ* IR spectroscopy are widely used technologies for real-time detection of reaction intermediates. Both RS and IR spectroscopy can detect the vibration modes of chemical bonds in molecules. The advancement of surface sensitive or enhanced RS or IR spectra making the detection of reaction intermediates more sensitive and accurate. IR spectroscopy and RS are complemental spectroscopic techniques. IR spectroscopy measures the absorption spectrum and RS measures the scattering spectrum. In many cases, the IR signal is stronger than RS signal. However, due to the sensitivity of infrared light to water molecules, the application of *in situ* IR in aqueous solution is challenging. RS can be operated in aqueous solutions, because the Raman scattering of water is very weak.

Dong[46] and colleagues used *in situ* shell-separated nanoparticles enhanced Raman spectroscopy (SHINERS) to systematically study the ORR reaction intermediates of the model system Pt(hkl) single crystal surface in the potential range of 1.1 V to 0.5 V (vs. RHE). For Pt(111), during the negative potential

drift, except for the peak at 933 cm^{-1}, there is no observable Raman signal in the range of 400 to 1,200 cm^{-1} until 0.8 V (vs. RHE) (Figure 4(A)). The peak at 933 cm^{-1} is attributed to the symmetric stretching mode of the perchlorate ion (ClO_4^-). When the potential drops to 0.6 V (vs. RHE), a clear Raman band appears at 732 cm^{-1}, and its intensity further increases as the potential decreases. Combined with the electrochemical results, the peak near 732 cm^{-1} is attributed to the O-O stretching vibration of $*O_2H$. Unlike Pt(111), when the potential decreases to 0.9 V (vs. RHE), the Raman peak of *OH appears at Pt(100) (Figure 4(B)), the peak of $*O_2H$ adsorbed on the surface is not observed. The phenomenon on the surface of Pt(110) is similar to that of Pt(100), but their relative Raman intensity and onset potential are different (Figure 4(C)). These data show that under acidic conditions, the ORR pathway on Pt(111) occurs through the formation of $*O_2H$, while on Pt(110) and Pt(100), it occurs through the formation of *OH. Different from the phenomenon in an acidic environment, three Pt(hkl) surfaces have the same superoxide intermediate species ($*O_2^-$) in an alkaline condition (Figure 4(D-F)).

In situ IR spectroscopy is also a powerful tool for identifying reaction intermediates. Nayak et al.[32] have revealed the infrared spectrum of the Pt/C model catalyst recorded under O_2 in the 0.1 mol·L^{-1} $HClO_4$ electrolyte (Figure 4(G)). The band at 1212 cm^{-1} is designated as the O-O stretching mode of surface adsorption superoxide ($*O_2H$); the 1386 cm^{-1} band is attributed to the O-O-H bending mode of the surface adsorbed hydroperoxide (*HOOH), and the 1468 cm^{-1} band is attributed to the O-O stretching mode of weakly adsorbed molecular oxygen ($*O_2$). The adsorbed superoxide ($*O_2H$) exists at a potential as high as 0.9 V (vs. RHE), while the adsorbed hydroperoxide (*HOOH) is only observed below the onset potential of ORR.

Wang[38] et al. also used SHINERS to study reaction intermediates of the alloy model systems Pt_3Co at different pH values. Under alkaline conditions, at potentials below 0.7 V (vs. RHE), the two peaks at 711 and 876 cm^{-1} are assigned to the adsorptions of $*O_2H$ and $*O_2^-$. Under alkaline conditions, when the potential is lower than 0.7 V (vs. RHE), a broad peak with shoulders appears, which can be divided into two Raman bands (698 and 750 cm^{-1}). The band at 698 cm^{-1} is compared with the one measured ($*O_2H$) in acid. With the help of DFT calculations, the new band at 750 cm^{-1} is attributed to the OH adsorbed on Co, which indicates that Co can coexist with Pt on the surface under alkaline conditions (Figure 4(I)). However, in an acidic environment, metal Co in the alloy will be leached and the *OH signal will disappear (Figure 4(H)). *In situ* transmission electron microscopy also showed Co segregation. Therefore, the significant *OH adsorption and Co segregation result in the performance of Pt_3Co in alkaline solutions slightly lower than in acidic solutions.

3.2 Molecular Catalysts

The adsorption of reactants, the reaction, and the desorption of products are elemental steps in catalytic systems. The direct imaging of the reactants and intermediates on catalytic center can provide direct evidence for the catalytic processes. For example, the adsorption of O_2 on the $M\text{-}N_4$ site is widely regarded as the initial step of transition metal porphyrins (MPs) and transition metal phthalocyanines (MPcs) -based molecular materials catalyzed ORR. The interaction between O_2 and the catalyst results in a change in the contrast of the adsorbed species, which can be observed in the STM image.

There have been many *ex situ* studies that have identified various O_2 related species from STM images. Friesenet[47] et al. used STM to study the combination of O_2 and CoOEP on HOPG. The bright and dim species can be observed in the STM image at the same time, and the dim species is identified as CoOEP-O_2 species. In addition to O_2 adsorption, O atom adsorption can also be observed in some systems. For example, Hulsken[48] et al. found that high contrast Mn-O species can be observed in the STM image of the Mn porphyrin monolayer. These studies are the basis for the species attribution in species evolution during the reaction process.

STM has been widely used for *in situ* characterization of the catalytic ORR process in molecular model

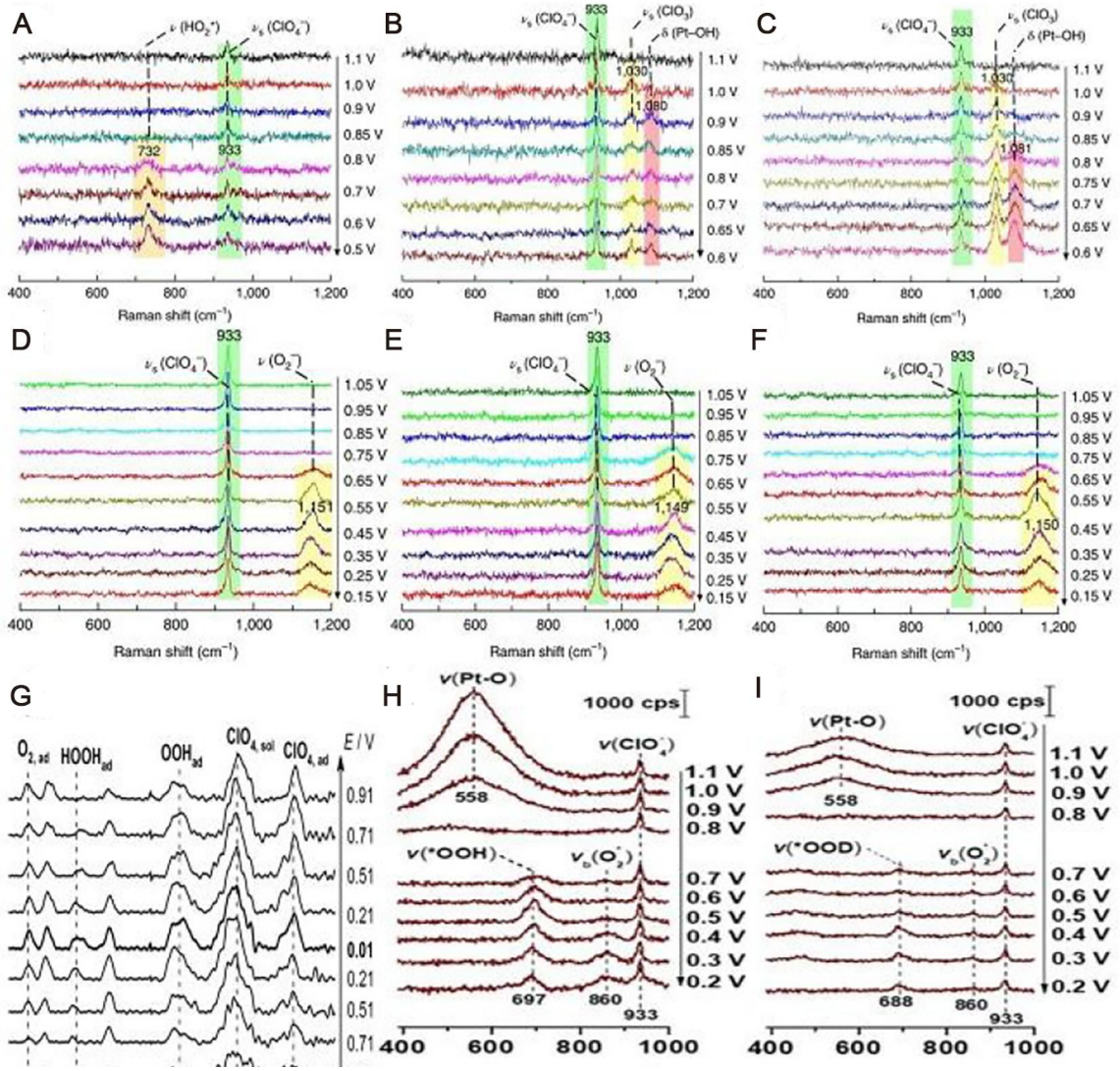

Figure 4 (A) SHINERS spectra of the ORR system at a Pt(111) electrode surface in a 0.1 mol·L^{-1} $HClO_4$ solution saturated with O_2. (B) SHINERS spectra of the ORR at a Pt(100) electrode surface in a 0.1 mol·L^{-1} $HClO_4$ solution. (C) SHINERS spectra of the ORR at a Pt(100) electrode surface in a 0.1 mol·L^{-1} $HClO_4$ solution. (D) SHINERS spectra of the ORR system at a Pt(111) electrode surface in 0.1 mol·L^{-1} $NaClO_4$ solution (pH of approximately 10.3) saturated with O_2. (E) SHINERS spectra of the ORR at a Pt(100) electrode surface in 0.1 mol·L^{-1} $NaClO_4$ solution (pH of approximately 10.3) saturated with O_2. (F) SHINERS spectra of the ORR at a Pt(100) electrode surface in 0.1 mol·L^{-1} $NaClO_4$ solution (pH of approximately 10.3) saturated with O_2. (G) *In situ* IR spectra of Pt/C during ORR in 0.1 mol·L^{-1} $HClO_4$ solution. (H) *In situ* SHINERS spectra of ORR on dealloyed Pt_3Co nanocatalysts in 0.1 mol·L^{-1} O_2-saturated $HClO_4$ solution. (I) *In situ* SHINERS spectra of the ORR on dealloyed Pt_3Co nanocatalysts in O_2-saturated 0.1 mol·L^{-1} $NaClO_4$ + 0.001 mol·L^{-1} NaOH solutions. (A-F) Reproduced from Ref[46]. With permission from the Nature Energy. (G) Reproduced from Ref[32]. With permission from the Wiley Online Library. (H-I) Reproduced from Ref[38]. With permission from the Wiley Online Library. (color on line)

systems. Under the different potentials of the ORR reaction, the arrangement, contour and contrast of the adsorbed species can be observed in the STM image. Gu et al.[49] used *in situ* ECSTM to study the ORR catalyzed by iron (II) phthalocyanine (FePc), and observe the process of FePc molecule catalyzed ORR. In the initial stage of the catalytic ORR, FePc molecules can combine with O_2 molecules to form a high-contrast FePc-O_2 complex. The number of such high-contrast FePc-O_2 complexes increase with the increase

of the oxygen content in the solution. After the ORR reaction is turned on by the potential, the high-contrast FePc-O_2 complex is immediately transformed into the low-contrast FePc molecule, as shown in Figure 5 (A, B). The theoretical simulation results also confirmed the occurrence of this process. Cai[50] et al. also used *in situ* ECSTM to study the ORR catalyzed by tetraphenyl cobalt porphyrin (CoTPP), and observed the conversion process between the active intermediate CoTPP-O_2 complex and the catalyst. The results provide *in situ* experimental evidence for the study of the catalytic reaction mechanism and catalytic active sites of MPs/MPcs molecular materials in the ORR process.

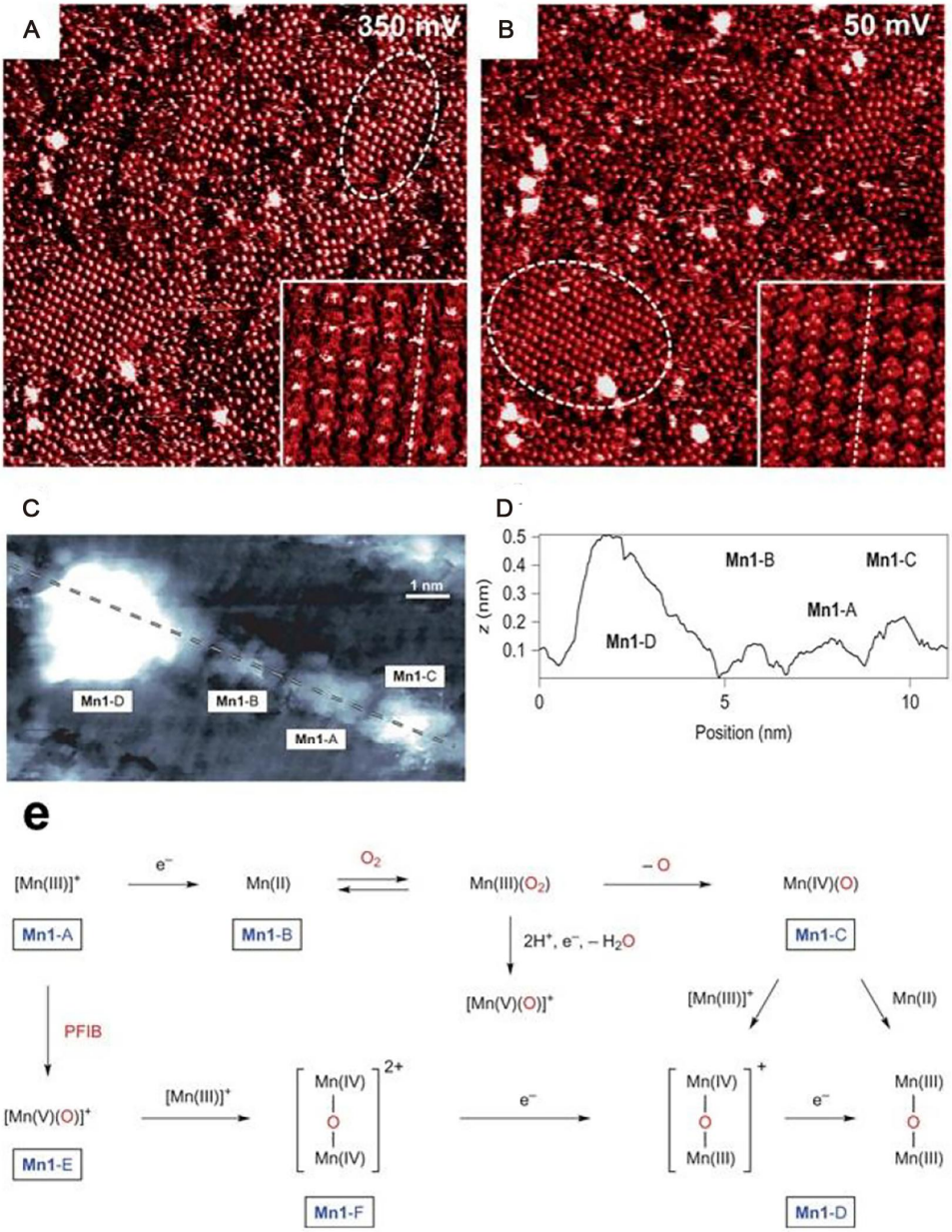

Figure 5 (A-B) *In situ* STM images of FePc on Au(111) in O_2-saturated 0.1 mol·L^{-1} $HClO_4$: (A) ORR off; (B) ORR on. (C-D) STM topographic image (C) and cross-section analysis (D) of Mn1Cl at the HOPG/1-octanoic acid interface under ambient conditions; (E) Possible pathways and states of the manganese centre of Mn-porphyrins during their reaction with O_2. (A-B) Reproduced from Ref[49]. With permission from the American Chemical Society. (C-E) Reproduced from Ref[50]. With permission from the Nature Chemistry. (color on line)

Boer et al.[51] used a Mn porphyrin derivative (called Mn1Cl) as a model system, and successfully observed several intermediates produced by Mn1Cl in the process of catalytic oxygen reduction at the solid-liquid interface. As shown in Figure 5(C, D), at the octanoic acid /graphite interface, Mn1Cl molecules present four states with significantly different contrasts, which are labeled by Mn1-A, Mn1-B, Mn1-C, and Mn1-D. The height of these four species in the longitudinal direction of the analysis also corresponds to four different heights. These species with different contrasts can exist stably for several minutes or even several hours during the imaging process. Through further atmospheric control experiments and statistical analysis, the author classified Mn1-A as a reactant, while Mn1Cl, Mn1-B, Mn1-C, and Mn1-D are respectively classified as different reaction intermediates, and a schematic diagram of the reaction mechanism of this process is given in Figure 5(E).

4 Conclusions and outlooks

In situ characterization is playing an increasingly important role in the field of electrocatalysis. Through real-time detection of catalysts, reactants and reaction intermediates, the dynamic process of O_2 reduction reaction (ORR) can be clearly revealed, which helps to accurately understand the catalytic mechanism. In this article, we elaborate on the *in situ* research progress in exploring the evolution of catalysts in the O_2 reduction process. In addition, we also summarize *in situ* studies on monitoring O_2 reduction reactants, reaction intermediates and catalytic processes.

ORR is a complex multi-electron process. Combining two or more *in situ* technologies provide a more comprehensive picture for the reaction mechanism. For example, the combination of *in situ* IR spectroscopy, RS and XAS can obtain surface-specific chemical information, including the local coordination environment, and structure and oxidation state of the electrocatalyst during the catalysis process. *In situ* STM can provide the evolution of adsorbed species during ORR. Combined with theoretical calculations, it is possible to have a more comprehensive understanding of the basic process and a deeper understanding of the reaction mechanism.

One increasingly important aspect in *in situ* characterization is the development of the time-resolved and spatially-resolved technology. Using high time-resolved and spatially-resolved techniques to study the catalytic reaction process can reveal the existence of shortly-lived intermediates, determine the reaction rate-limiting steps, provide a basis for the catalytic mechanism of the catalyst, and help reveal the catalytic reaction pathway. For example, video-STM[52,53] with atomic spatial resolution and millisecond time resolution can be performed in an aqueous solution to reveal the diffusion behaviors of the adsorbent on the electrode surface in electrocatalysis on the atomic scale. In principle, XAS can also track faster catalytic progress. There have been some known successful examples where synchrotron-based XAS[54] has been used to monitor the kinetics of the catalyst process on a time scale of hundreds of picoseconds. In addition, the reactivity map of the catalyst surface can be obtained by scanning electrochemical microscopy (SECM). The spatial resolution of SECM is related to the tip size and has been improved significantly in recent years. A recently developed new method scanning electrochemical cell microscopy (SECCM) can probe a highly spatially-resolved catalytic process for ORR of Pt clusters and nanoparticles, and the catalytic activity can be revealed[55].

Another important developing direction of *in situ* characterization is the combination of these *in situ* techniques to resolve the electrocatalytic from different aspects. For instance, the combination of STM and spectroscopic techniques provides a comprehensive characterization for the identification of the structural information and chemical information of the electrocatalytic system. Tip-enhanced Raman spectroscopy (TERS) combines the high spatial resolution of STM with the chemical discrimination capability of RS. Electrochemical TERS (EC-TERS) can be operated in an aqueous solution to directly study the structure-activity relationship of electrocatalysts. Su et al.[56] used EC-TERS to study the atomic site-specific electronic properties of Pt adatoms with

different coordination numbers, which provided in sights into the relationship between the electrocatalytic behavior of Pt catalysts and the localized surface nanostructure. In addition, the combination of STM and SECM can obtain spatially resolved electrochemical activity information on the catalyst surface. Patrick R. Unwin[57] has realized conductance and electron tunneling SECM on the surface of Au nanocrystal electrodes. The simultaneous mapping of the substrate topography and electrochemical activity can be achieved. In summary, the *in situ* characterization of ORR has developed rapidly in recent years. With the deepening of *in situ* technology, there will be more exciting results in the research of electrocatalytic reactions.

Acknowledgements:

This work is supported by the National Key R&D Program of China (2017YFA0204702) and the National Natural Science Foundation of China (Grant No. 21725306, and 21972147).

References:

[1] Sharaf O Z, Orhan, M F. An overview of fuel cell technology: Fundamentals and applications[J]. Renew. Sust. Enegy Rev., 2014, 32: 810-853.

[2] Steele B C H, Heinzel A. Materials for fuel-cell technologies[J]. Nature, 2001, 414(6861): 345-352.

[3] Debe M K. Electrocatalyst approaches and challenges for automotive fuel cells[J]. Nature, 2012, 486(7401): 43-51.

[4] Badwal S P S, Giddey S, Kulkarni A, Goel J, Basu S. Direct ethanol fuel cells for transport and stationary applications-A comprehensive review[J]. Appl. Energ., 2015, 145: 80-103.

[5] Wang W, Su C, Wu Y Z, Ran R, Shao Z P. Progress in solid oxide fuel cells with nickel-based anodes operating on methane and related fuels[J]. Chem. Rev., 2013, 113(10): 8104-8151.

[6] Wu G, More K L, Johnston C M, Zelenay P. High-performance electrocatalysts for oxygen reduction derived from polyaniline, iron, and cobalt[J]. Science, 2011, 332(6028): 443-447.

[7] Kuttiyiel K A, Sasaki K, Su D, Wu L J, Zhu Y M, Adzic R R. Gold-promoted structurally ordered intermetallic palladium cobalt nanoparticles for the oxygen reduction reaction[J]. Nat. Commun., 2014, 5: 5185.

[8] Lu Y Z, Jiang Y Y, Gao X H, Wang X D, Chen W. Strongly coupled Pd nanotetrahedron/tungsten oxide nanosheet hybrids with enhanced catalytic activity and sability as oxygen reduction electrocatalysts[J]. J. Am. Chem. Soc., 2014, 136(33): 11687-11697.

[9] Savadogo O, Lee K, Oishi K, Mitsushima S, Kamiya N, Ota K I. New palladium alloys catalyst for the oxygen reduction reaction in an acid medium[J]. Electrochem. Commun., 2004, 6(2): 105-109.

[10] Wang X, Choi S I, Roling L T, Luo M, Ma C, Zhang L, Chi M F, Liu J Y, Xie Z X, Herron J A, Mavrikakis M, Xia Y N. Palladium-platinum core-shell icosahedra with substantially enhanced activity and durability towards oxygen reduction[J]. Nat. Commun., 2015, 6: 7594.

[11] Miner, E M, Fukushima, T, Sheberla, D, Sun L, Surendranath Y, Dinca M. Electro-chemical oxygen reduction catalysed by Ni_3(hexaimino-triphenylene)$_2$[J]. Nat. Commun., 2016, 7:10942.

[12] Masa J, Xia W, Muhler M, Schuhmann W. On the role of metals in nitrogen-doped carbon electrocatalysts for oxygen reduction[J]. Angew. Chem. Int. Edit., 2015,54(35): 10102-10120.

[13] Tang H J, Yin H J, Wang J Y, Yang N L, Wang D, Tang Z Y. Molecular architecture of cobalt porphyrin multilayers on reduced graphene oxide sheets for high-performance oxygen reduction reaction[J]. Angew. Chem. Int. Edit., 2013, 52(21): 5585-5589.

[14] Ding K Q, Cheng F M. Cyclic voltammetrically prepared MnO_2-PPy composite material and its electrocatalysis towards oxygen reduction reaction (ORR)[J]. Synthetic Met., 2009, 159(19-20): 2122-2127.

[15] Allen C J, Hwang J, Kautz R, Mukerjee S, Plichta E J, Hendrickson M A, Abraham K M. Oxygen reduction reactions in ionic liquids and the formulation of a general ORR mechanism for Li-air batteries[J]. J. Phys. Chem. C, 2012, 116(39): 20755-20764.

[16] Roche I, Chaĭnet E, Chatenet M, Vondrak J. Carbon-supported manganese oxide nanoparticles as electrocatalysts for the oxygen reduction reaction (ORR) in alkaline medium: physical characterizations and ORR mechanism[J]. J. Phys. Chem. C, 2007, 111(3): 1434-1443.

[17] Kuang F, Zhang D, Li Y J, Wan Y, Hou B R. Electrochemical impedance spectroscopy analysis for oxygen reduction reaction in 3.5% NaCl solution[J]. J. Solid State Electr., 2009, 13(3): 385-390.

[18] Queuedo M C, Galicia G, Mayen-Mondragon R, Llongueras J G. Role of turbulent flow seawater in the corrosion enhancement of an Al-Zn-Mg alloy: an electrochemical

impedance spectroscopy (EIS) analysis of oxygen reduction reaction (ORR)[J]. J. Mater. Res. Technol., 2018, 7(2): 149-157.

[19] Feng L Y, Liu Y J, Zhao J X. Iron-embedded boron nitride nanosheet as a promising electrocatalyst for the oxygen reduction reaction (ORR): a density functional theory (DFT) study[J]. J. Power Sources, 2015, 287: 431-438.

[20] Seifitokaldani A, Savadogo O, Perrier M. Density functional theory (DFT) computation of the oxygen reduction reaction (ORR) on titanium nitride (TiN) surface[J]. Electrochim. Acta., 2014, 141: 25-32.

[21] Subbaraman R, Danilovic N, Lopes P P, Tripkovic D, Strmcnik D, Stamenkovic V R, Markovic N M. Origin of anomalous activities for electrocatalysts in alkaline electrolytes[J]. J. Phys. Chem. C, 2012, 116(42): 22231-22237.

[22] Li D G, Wang C, Strmcnik D S, Strmcnik D S, Tripkovic D V, Sun X L, Kang Y J, Chi M F, Snyder J D, van der Vliet D, Tsai Y F, Stamenkovic V R, Sun S H, Markovic N M. Functional links between Pt single crystal morphology and nanoparticles with different size and shape: the oxygen reduction reaction case[J]. Energ. Environ. Sci., 2014, 7(12): 4061-4069.

[23] Wan L J, Moriyama T, Ito M, Uchida H, Watanabe M. *In situ* STM imaging of surface dissolution and rearrangement of a Pt-Fe alloy electrocatalyst in electrolyte solution[J]. Chem. Commun., 2002(1): 58-59.

[24] Todoroki N, Iijima Y, Takahashi R, Asakimori Y, Wadayama T. Structure and electrochemical stability of Pt-enriched Ni/Pt(111) topmost surface prepared by molecular beam epitaxy[J]. J. Electrochem. Soc., 2013, 160(6): F591-F596.

[25] Yoshimoto S, Tada A, Itaya K. *In situ* scanning tunneling microscopy study of the effect of iron octaethylporphyrin adlayer on the electrocatalytic reduction of O_2 on Au (111)[J]. J. Phys. Chem. B, 2004, 108(17): 5171-5174.

[26] Gocyla M, Kuehl S, Shviro M, Heyen H, Selve S, Dunin-Borkowski R E, Heggen M, Strasser P . Shape stability of octahedral PtNi nanocatalysts for electrochemical oxygen reduction reaction studied by *in situ* transmission electron microscopy[J]. ACS Nano, 2018, 12(6): 5306-5311.

[27] Gatalo M, Ruiz-Zepeda F, Hodnik N, Drazic G, Bele M, Gaberscek M. Insights into thermal annealing of highly-active $PtCu_3$/C oxygen reduction reaction electrocatalyst: An *in situ* heating transmission electron microscopy study[J]. Nano Energy, 2019, 63: 103892.

[28] Strickland K, Miner E, Jia Q, Tylus U, Ramaswamy N, Liang W T, Sougrati M T, Jaouen F, Mukerjee S. Highly active oxygen reduction non-platinum group metal electrocatalyst without direct metal-nitrogen coordination[J]. Nat. Commun., 2015, 6: 7343.

[29] Lima F H B, Calegaro M L, Ticianelli E A. Electrocatalytic activity of manganese oxides prepared by thermal decomposition for oxygen reduction[J]. Electrochim. Acta., 2007, 52(11): 3732-3738.

[30] Celorrio V, Leach A S, Huang H L, Hayama S, Freeman A, Inwood D W, Fermin D J, Russell A E. Relationship between Mn oxidation state changes and oxygen reduction activity in (La, Ca) MnO_3 as probed by *in situ* XAS and XES[J]. ACS Catal., 2021, 11(11): 6431-6439.

[31] Merte L R, Behafarid F, Miller D J, Friebel D, Cho S, Mbuga F, Sokaras D, Alonso-Mori R, Weng T C, Nordlund D. Electrochemical oxidation of size-selected Pt nanoparticles studied using *in situ* high-energy-resolution X-ray absorption spectroscopy[J]. ACS Catal., 2012, 2(11): 2371-2376.

[32] Nayak S, McPherson I J, Vincent K A. Adsorbed intermediates in oxygen reduction on platinum nanoparticles observed by *in situ* IR spectroscopy[J]. Angew. Chem. Int. Edit., 2018, 57(39): 12855-12858.

[33] Shao M H, Liu P, Adzic R R. Superoxide anion is the intermediate in the oxygen reduction reaction on platinum electrodes[J]. J. Am. Chem. Soc., 2006, 128(23): 7408-7409.

[34] Baranton S, Coutanceau C, Garnier E, Leger J M. How does α-FePc catalysts dispersed onto high specific surface carbon support work towards oxygen reduction reaction (ORR)?[J]. J. Electroanal. Chem., 2006, 590(1): 100-110.

[35] Nayak S, Biedermann P U, Stratmann M, Erbe A. A mechanistic study of the electrochemical oxygen reduction on the model semiconductor n-Ge(100) by ATR-IR and DFT[J]. Phys. Chem. Chem. Phys., 2013, 15(16): 5771-5781.

[36] Frith J T, Russell A E, Garcia-Araez N, Owen J R. An *in situ* Raman study of the oxygen reduction reaction in ionic liquids[J]. Electrochem. Commun., 2014, 46: 33-35.

[37] Sugimura F, Sakai N, Nakamura T, Nakamura M, Ikeda K, Sakai T, Hoshi N. *In situ* observation of Pt oxides on the low index planes of Pt using surface enhanced Raman spectroscopy[J]. Phys. Chem. Chem. Phys., 2017, 19(40): 27570-27579.

[38] Wang Y H, Le J B, Li W Q, Wei J, Radjenovic P M, Zhang H, Zhou X S, Cheng J, Tian Z Q, Li J F. *In situ* spectroscopic insight into the origin of the enhanced performance of bimetallic nanocatalysts towards the oxygen reduction reaction (ORR)[J]. Angew. Chem. Int. Ed., 2019, 58(45): 16062-16066.

[39] Ze H J, Chen X, Wang X T, Wang Y H , Chen Q Q, Lin J S, Zhang Y J, Zhang X G, Tian Z Q, Li J F. Molecular insight of the critical role of Ni in Pt-based nanocatalysts for improving the oxygen reduction reaction probed using an *in situ* SERS borrowing strategy[J]. J. Am. Chem. Soc., 2021, 143(3): 1318-1322.

[40] Dong J C, Su M, Briega-Martos V, Li L, Le J B, Radjenovic P, Zhou X S, Feliu J M, Tian Z Q, Li J F. Direct *in situ* Raman spectroscopic evidence of oxygen reduction reaction intermediates at high-index Pt (hkl) surfaces[J]. J. Am. Chem. Soc., 2019, 142(2): 715-719.

[41] Wu J F, Shan S Y, Petkov V, Prasai B, Cronk H, Joseph P, Luo J, Zhong C J. Composition-structure-activity relationships for palladium-alloyed nanocatalysts in oxygen reduction reaction: an *ex-situ*/*in situ* high energy X-ray diffraction study[J]. ACS Catal., 2015, 5(9): 5317-5327.

[42] Zhu G Z, Prabhudev S, Yang J, Gabardo C M, Botton G A, Soleymani L. *In situ* liquid cell TEM study of morphological evolution and degradation of Pt-Fe nanocatalysts during potential cycling[J]. J. Phys. Chem. C, 2014, 118(38): 22111-22119.

[43] Brenet J P. Electrochemical behaviour of metallic oxides [J]. J. Power Sources, 1979, 4(3): 183-190.

[44] Mao L Q, Zhang D, Sotomura T, Nakatsu K, Koshiba N, Ohsaka T. Mechanistic study of the reduction of oxygen in air electrode with manganese oxides as electrocatalysts [J]. Electrochim. Acta., 2003, 48(8): 1015-1021.

[45] Qin H Y, Lin L X, Jia J K, Ni H L, He Y, Wang J, Li A G, Ji Z G, Liu J B. Synchrotron radiation *in situ* X-ray absorption fine structure and *in situ* X-ray diffraction analysis of a high-performance cobalt catalyst towards the oxygen reduction reaction[J]. Phys. Chem. Chem. Phys., 2017, 19(45): 30749-30755.

[46] Dong J C, Zhang X G, Briega-Martos V, Jin X, Yang J, Chen S, Yang Z L, Wu D Y, Feliu J M, Williams C T, Tian Z Q, Li J F. *In situ* Raman spectroscopic evidence for oxygen reduction reaction intermediates at platinum single-crystal surfaces[J]. Nat. Energy, 2019, 4(1): 60-67.

[47] Friesen B A, Bhattarai A, Mazur U, Hipps K W. Single molecule imaging of oxygenation of cobalt octaethylporphyrin at the solution/solid interface: thermodynamics from microscopy[J]. J. Am. Chem. Soc., 2012, 134(36): 14897-14904.

[48] Hulsken B, Van Hameren R, Gerritsen J W, Khoury T, Thordarson P, Crossley M J, Rowan A E, Nolte R J M, Elemans J A A W, Speller S. Real-time single-molecule imaging of oxidation catalysis at a liquid-solid interface [J]. Nat. Nanotechnol., 2007, 2(5): 285-289.

[49] Gu J Y, Cai Z F, Wang D, Wang L J. Single-molecule imaging of iron-phthalocyanine-catalyzed oxygen reduction reaction by *in situ* scanning tunneling microscopy[J]. ACS Nano, 2016, 10(9): 8746-8750.

[50] Cai Z F, Wang X, Wang D, Wang L J. Cobalt-porphyrin-catalyzed oxygen reduction reaction: A scanning tunneling microscopy study[J]. ChemElectroChem, 2016, 3(12): 2048-2051.

[51] Den Boer D, Li M, Habets T, Iavicoli P, Rowan A E, Nolte R J M, Speller S, Amabilino D B, De Feyter S, Elemans J A A W. Detection of different oxidation states of individual manganese porphyrins during their reaction with oxygen at a solid/liquid interface[J]. Nat. Chem., 2013, 5(7): 621-627.

[52] Patera L L, Bianchini F, Africh C, Dri C, Soldano G, Mariscal M M, Peressi M, Comelli G. Real-time imaging of adatom-promoted graphene growth on nickel[J]. Science, 2018, 359(6381): 1243-1246.

[53] Rahn B, Magnussen O M. Sulfide surface dynamics on Cu(100) and Ag(100) electrodes in the presence of c (2×2) halide adlayers[J]. ChemElectroChem, 2018, 5(20): 3073-3082.

[54] Borfecchia E, Garino C, Gianolio D, Salassa L, Gobetto R, Lamberti C. Monitoring excited state dynamics in cis-$[Ru(bpy)_2(py)_2]^{2+}$ by ultrafast synchrotron techniques[J]. Catal. Today., 2014, 229: 34-45.

[55] Ustarroz J, Ornelas I M, Zhang G H, Perry D, Kang M, Bentley C L, Walker M, Unwin P R. Mobility and poisoning of mass-selected platinum nanoclusters during the oxygen reduction reaction[J]. ACS Catal., 2018, 8(8): 6775-6790.

[56] Su H S, Zhang X G, Sun J J, Jin X, Wu D Y, Lian X B, Zhong J H, Ren B. Real-space observation of atomic site-specific electronic properties of a Pt nanoisland/Au(111) bimetallic surface by tip-enhanced Raman spectroscopy [J]. Angew. Chem. Int. Ed., 2018, 57(40): 13177-13181.

[57] Edmondson J F, Meloni G N, Costantini G, Unwin P R. Synchronous electrical conductance-and electron tunnelling-scanning electrochemical microscopy measurements[J]. ChemElectroChem, 2020, 7(3): 697-706.

电催化氧还原反应的原位表征

冯雅辰[1,2],王 翔[1,2],王宇琪[1,2],严会娟[1,2],王 栋[1,2*]

(1. 中国科学院分子纳米结构与纳米技术重点实验室,北京分子科学国家研究中心,中国科学院化学研究所,北京 100190; 2. 中国科学院大学,北京 100049)

摘要: 燃料电池作为一种电化学能量转换系统,具有能量转换效率高、清洁度高等优点。氧还原反应(ORR)是燃料电池中重要的阴极反应。目前,电催化剂仍是制约燃料电池进一步商业化的关键材料之一。ORR 反应催化机理的研究对于开发具有良好活性和高选择性的电催化剂具有重要价值。近年来人们通过各种先进的原位表征方法深入研究了 ORR 催化剂的机理和催化过程。本综述旨在总结用于原位表征技术应用于研究 ORR 反应机制的最新研究进展。我们首先简要介绍各种原位技术在 ORR 研究中的优势,包括电化学扫描隧道技术、红外光谱、拉曼光谱、X 射线吸收光谱、X 射线衍和透射电子显微镜等。然后,从催化剂的角度,总结了各种原位表征技术在催化剂形貌和电子结构演变以及催化过程中反应物和中间体的识别中的应用。最后,展望讨论了该领域原位技术的未来发展。

关键词: 氧还原反应;原位表征;电催化过程